21st AIAA Aerodynamic Decelerator Systems Technology Conference and Seminar
23 - 26 May 2011, Dublin, Ireland

AIAA 2011-2509

# Subscale Test Program for the Orion Conical Ribbon Drogue Parachute

Anita Sengupta[*]
*Jet Propulsion Laboratory, California Institute of Technology, Pasadena, CA, 91109*

Phil Stuart[†], Ricardo Machin[‡], Gary Bourland[†], Alan Schwing[†]
*NASA Johnson Space Center, Houston, TX, 77058*

Ellen Longmire[§]
*University of Minnesota, Minneapolis, MN*

Elsa Hennings[**]
*US Navy, China Lake, CA, 93555*

Robert Sinclair[††]
*Airborne Systems, Santa Ana, CA, 92704*

**A subscale wind tunnel test program for Orion's conical ribbon drogue parachute is under development. The desired goals of the program are to quantify aerodynamic performance of the parachute in the wake of the entry vehicle, including understanding of the coupling of the parachute and command module dynamics, and an improved understanding of the load distribution within the textile elements of the parachute. The test program is conducted in a 3x2.1 m (10x7 ft) closed loop subsonic wind tunnel. The subscale test program is uniquely suited to probing the aerodynamic and structural environment in both a quantitative and qualitative manner. Non-intrusive diagnostics, including Particle Image Velocimetry for wake velocity surveys, high speed pressure transducers for canopy pressure distribution, and a high speed photogrammetric reconstruction, will be used to quantify the parachute's performance.**

## Nomenclature

| | | |
|---|---|---|
| $D_o$ | = | Parachute nominal diameter |
| $d$ | = | Command module maximum diameter |
| $x/d$ | = | Non-dimensional trailing distance |
| $C_D$ | = | Drag coefficient |
| $q$ | = | Dynamic Pressure |
| $Re$ | = | Reynolds number |
| $\alpha$ | = | Angle of attack |
| $T_{inf}$ | = | Free stream temperature |
| $\rho$ | = | Density |
| $\mu$ | = | Viscosity |
| $T_{inf}$ | = | Free stream temperature |
| $S_o$ | = | Parachute nominal area |

[*] Senior Engineer, Systems Engineering, MS-301-365, Senior Member.
[†] Aerospace Engineer, Aerosciences and Flight Mechanics Branch, MC EG3.
[‡] Chief Engineer, Aerosciences and Flight Mechanics Branch, MC EG3, Member.
[§] Professor, Department of Aerospace Engineering.
[**] Chief Engineer, Warfighter Systems and Support Division, Code 466000D, Associate Fellow.
[††] Chief Engineer, Space Systems Business Unit, Associate Fellow.

## I. Introduction

The high cost of full-scale testing, as well as the need for validation data for computational tools, motivate the use of sub-scale test facilities and approaches for the design of Earth-based deceleration systems. A subscale test program is uniquely suited to probing the aerodynamic and structural environments in both a quantitative and qualitative manner. Prior experience and usefulness of testing subscale parachutes for extraterrestrial applications: Huygens, Mars Exploration Rovers (MER), and Mars Science Laboratory (MSL); suggest this approach is valid and can be applied to the Earth Entry paradigm, as well. As such, a subscale test program for a conical ribbon drogue parachute, in the wake of the command module (CM), is under development for the Orion Crew Exploration Vehicle Parachute Assembly System (CPAS). The desired goals of the program are to quantify aerodynamic performance of the parachute in the wake of the entry vehicle, as well as optimization of the parachute in terms of load distribution, drag reduction mitigation, and dynamic response. The final aspect of the study is an assessment of the systems engineering level benefits that this approach achieves, including reduction in load prediction, mass allocation, and potential for drag performance improvements.

Traditional parachute testing consists of deploying a parachute from an aircraft at the appropriate deployment conditions with a streamlined parachute test vehicle (PTV), as shown in Figure 1 [1,2]. This type of test architecture allows assessment of the peak inflation load, drag performance, and reefing. This architecture usually does not match the aerodynamics of a manned or robotic re-entry mission, typically characterized by a blunt body payload. Similarly, dynamics driven by the blunt body interaction are also not captured.

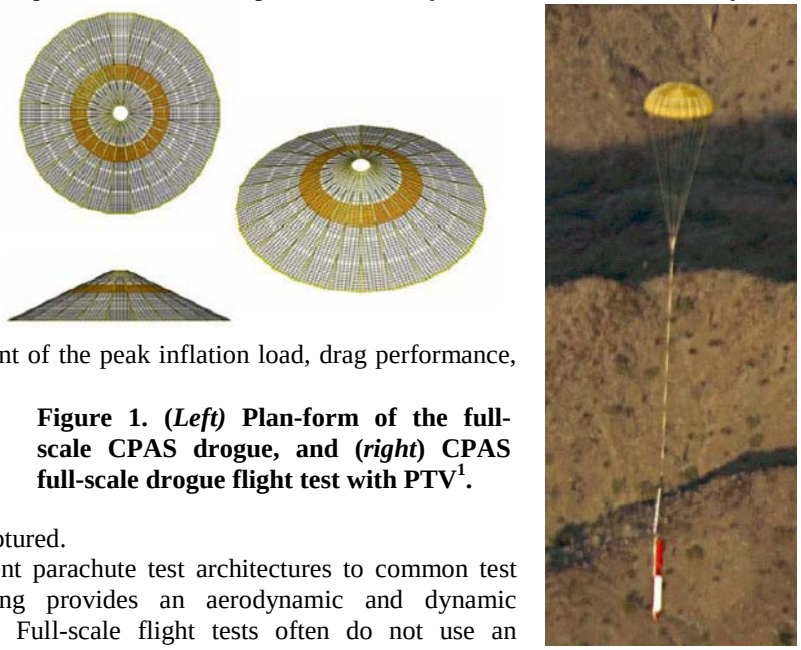

**Figure 1. (*Left)* Plan-form of the full-scale CPAS drogue, and (*right*) CPAS full-scale drogue flight test with PTV[1].**

Table 1 maps the attributes of current parachute test architectures to common test objectives. In general, subscale testing provides an aerodynamic and dynamic assessment, without load qualification. Full-scale flight tests often do not use an aerodynamically representative test vehicle (for blunt payloads), and therefore provide structural but not an accurate aerodynamic assessment.

Prior examples of subscale wind tunnel parachute testing are summarized in Table 2. The Viking Lander mission tested subscale parachutes to determine supersonic drag performance of the final parachute configuration[3]. The Army utilized a subscale test program to investigate performance of cross and quarter spherical parachutes[4]. MER utilized subscale subsonic wind tunnel tests to generate the aero database to quantify the effect of changes they made to the nominal Viking-type Disk-Gap-Band (DGB) design (variations in band and gap height) [5]. MSL conducted subscale wind tunnel tests to generate datasets to validate CFD and FSI codes and provide insight into the aerodynamics of DGB parachutes in supersonic flow[6]. Each of these test programs used different approaches to scaling the parachutes and deployment conditions.

**Table 1. Qualitative comparison of parachute test architecture attributes.**

| Test Architecture | Structural Assessment | Parachute Performance | Aerodynamic wake effect | Dynamic Wake Effect | Dynamic Model Validation | CFD validation dataset | Cost |
|---|---|---|---|---|---|---|---|
| Full Scale Flight w/o CM | Yes | Yes | No | No | No | No | Med |
| Full Scale with CM | Yes | Yes | Yes | Yes | Partial | Partial | High |
| Subscale Wind Tunnel | No | Yes | Yes | Yes | Yes | Yes | Low |
| Full Scale Wind Tunnel | Yes | Yes | Yes | Yes | Partial | Partial | Med |

**Table 2. Examples of subscale parachute tests.**

| Parameter | Viking | Huygens | Army | MER | MSL |
|---|---|---|---|---|---|
| Type | DGB | DGB,CR | Cross, Quarter Spherical | DGB | DGB |
| Scale (%) | 10 | --- | --- | 10 | 3 |
| Do (m) | 1.6 | 1.6 | 0.3 | 1.6 | 0.8 |
| Mach no. | 0.1-2.6 | 0.1-1.5 | <0.8 | 0.3-0.5 | 2-2.5 |
| q (kPa) | 4.7 | 4-6 | 0.015-0.2 | 1.2 | 4-19 |

## II. Wind Tunnel Testing Considerations

### A. Parachute performance

The parachute drag coefficient can be affected by the presence of a blunt-body wake. *Knacke* compiled the drag coefficient ($C_D$) loss for several subsonic parachute payload combinations as a function of the payload diameter *d* and trailing distance *x*. It exhibits a logarithmic decay with *x/d* [7].

$$\frac{C_D}{C_{D\infty}} = \frac{1}{5}\ln\left({}^{x}/_{d}\right) + \frac{2}{5} \quad (1)$$

Similarly, the parachute's dynamic stability and inflation may be affected by its interaction with the wake core resulting in failure to inflate, parachute collapse, unsteadiness, and other undesirable motions. An example would be the CPAS Cluster 2 test, where insufficient trailing distance, a result of capsule dynamics during the flight, likely led to the programmer chute collapse[8].

### B. Model Validation

Advances in computational tools and power allow parachute systems to be modeled by computational fluid dynamics (CFD), fluid structure interaction (FSI), and six-degree of freedom (6DOF) flight mechanics simulations. Collection of spatially and temporally resolved flow-field data can be used to validate these simulations, enhancing their fidelity and usefulness in the design process. Time resolved drag and pressure distribution measurements provide unique insight into textile design drivers, as well as validating membrane solvers and full FSI simulations.

### C. Wind Tunnel Test Scaling

Appropriate scaling is a critical part of all wind tunnel tests. Scaling has aerodynamic and fabrication implications. An inappropriate scaling of the test article can lead to a change in the magnitude of the effective length, i.e. a Reynolds number effect. Similarly, an inappropriately scaled test can lead to interaction of the test facility walls which can alter pressure and velocity distribution. Equally important is flow quality, namely steadiness and angularity which can introduce aerodynamic behavior non-representative of the flight application. From a fabrication perspective, scaling down a parachute can lead to changes in its inflated shape, stiffness, and porosity, which must be accounted for. Therefore, test scaling, fabrication, and facility selection must match the specific goals of the test.

#### *1. Reynolds Number*

Representing the wake accurately is essential for capturing the velocity deficit and recovery length, energy content, and coupling to the parachute flow field. All of these parameters have an effect on parachute pressure distribution and drag. The Reynolds (*Re*) number is the measure of the ratio of inertial to viscous forces in the flow. *Re* defines the flow regime (laminar or turbulent), which is particularly important for the blunt-body wake.

$$Re = \frac{\rho v d}{\mu} \quad (2)$$

The Orion capsule or command module (CM) is based on a large radius spherical heat-shield with a conical aft body, very similar to Apollo[9]. Its drag coefficient is a function of *Re*. The boundary layer over the forebody is known to be laminar for $Re<1.5x10^6$, therefore, to accurately capture the wake's effect on the parachute, a subscale test must exceed this value.

*2. Wind Tunnel Blockage*

A key parameter for any wind tunnel test is to determine the acceptable level of blockage. Blockage has two components, solid and wake. Solid blockage results from the physical reduction in open area due to the presence of the model. Wake blockage results from the viscous wake formed at the wall induced boundary layer [10].The result of blockage is that the flow speed near the model increases and pressure decreases (with respect to the free stream initial conditions), as shown in Figure 2. A correlation that is commonly used is the dynamic pressure correction ($q_{corr}$), a function of the blockage area ratio ($S_o/S_T$)[11].

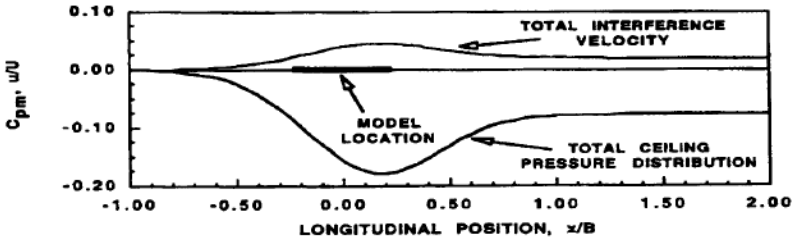


**Figure 2. Combined effect of solid and wake blockage effects on the pressure coefficient and velocity [10].**

$$\frac{q_{corr}}{q_{inf}} = 1 + 1.85\frac{C_D S_o}{S_T} \quad (3)$$

A series of computational fluid dynamic (CFD) simulations were performed to determine the effect of wind tunnel blockage on the CM wake and parachute drag. Overflow 2.1y, a Reynolds Averaged Navier Stokes (RANS) CFD code, was used to quantify blockage effects at 1,2,3,4 and 6% (Table 3). The computational grid included the wind tunnel walls, CM, and parachute. The drogue was represented by a thin disk at the projected diameter (4.9 m full scale). The disk was 6 *d* aft of the maximum diameter of the CM. A shear stress transport (SST) turbulence model and unsteady flow were used. The CM had a smooth, axis-symmetric outer mold line (Fig. 8). The simulated wind tunnel had a 3x2.1 m test section, inviscid walls, and 5 kPa free-stream dynamic pressure ($q$). All cases were run with a full-scale CM, yielding the correct *Re* for a 10% scale model, and test section dimensions scaled accordingly. This approach was chosen to separate blockage and Re effects in the results.

**Table 3. CFD simulation parameters.**

| Parameter | Value |
|---|---|
| Mach | 0.3 |
| α (deg) | 180 |
| $T_{inf}$ (K) | 288 |
| *Re* | $3x10^6$ |
| *x/d* | 6 |
| *q* (kPa) | 5 |

Figure 3 indicates the change in drag as a result of 1,2,3,4, and 6% blockage. The left figure shows the drag coefficient of the parachute, both in free-stream and behind the CM wake. The effect on the wake deficit is shown on the right. The results indicate that in the blockage range being considered, the effect on parachute and CM drag and flow field is minor and quantifiable.

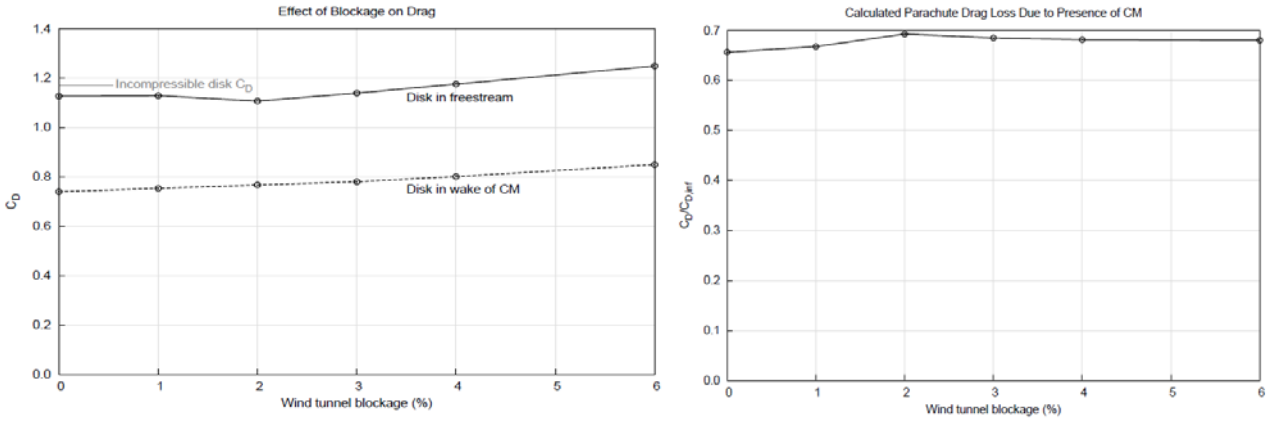


**Figure 3. CFD drag coefficient predictions. (*Left)* Comparison of parachute drag disk with and without the CM wake. (*Right*) The percent change in drag due to blockage.**

Figure 4 shows contour plots of $q/q_{inf}$ for the parachute (disk) only. This case was used to generate the chute alone drag variation due to blockage. The parachute's wake becomes more truncated and streamlined with

increasing blockage but the cross-stream gradient in dynamic pressure is similar up to 5% blockage. Figure 5 are contour plots of $q/q_{inf}$ in the pitch plane for the CM with the trailing parachute. The local $q$ and wake width near the CM changes with increasing blockage. Specifically the CM wake core becomes more truncated with increasing blockage. However, the overall effect on canopy pressure distribution was minimal (from 1% to 6% blockage).

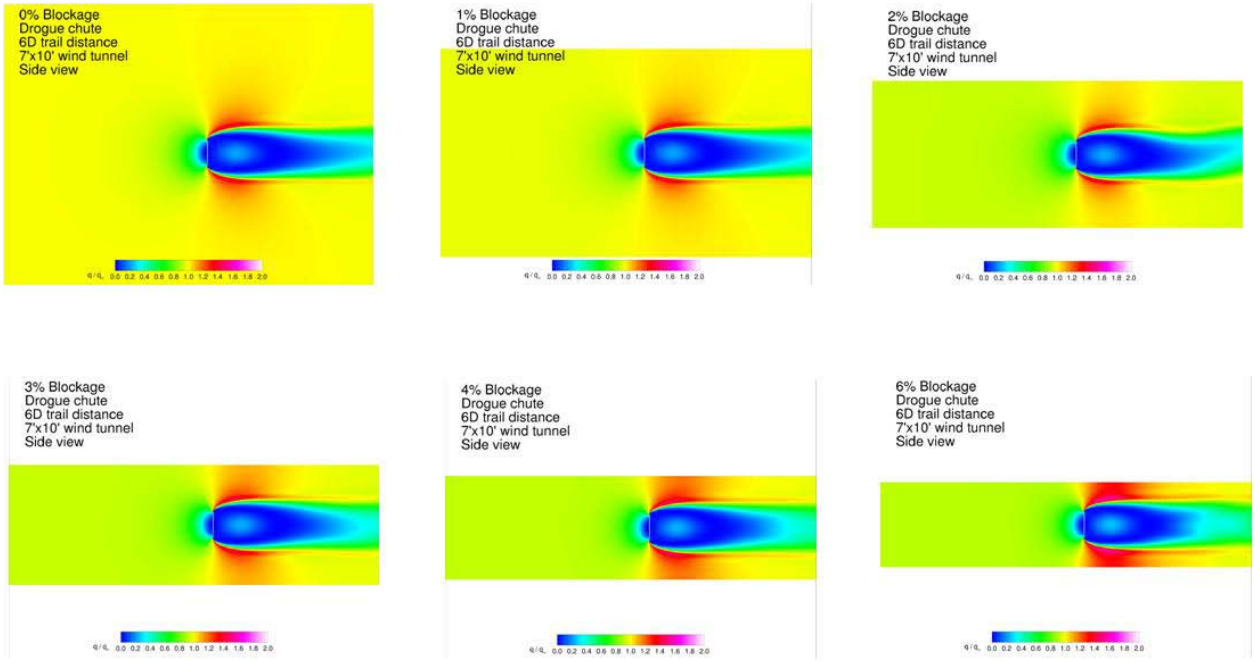


**Figure 4. Contours of normalized dynamic pressure ($q/q_{inf}$) for the CM wake flow field at Re=3x10$^6$ at (*from left to right*) 1,2,3,4, and 6% blockage.**

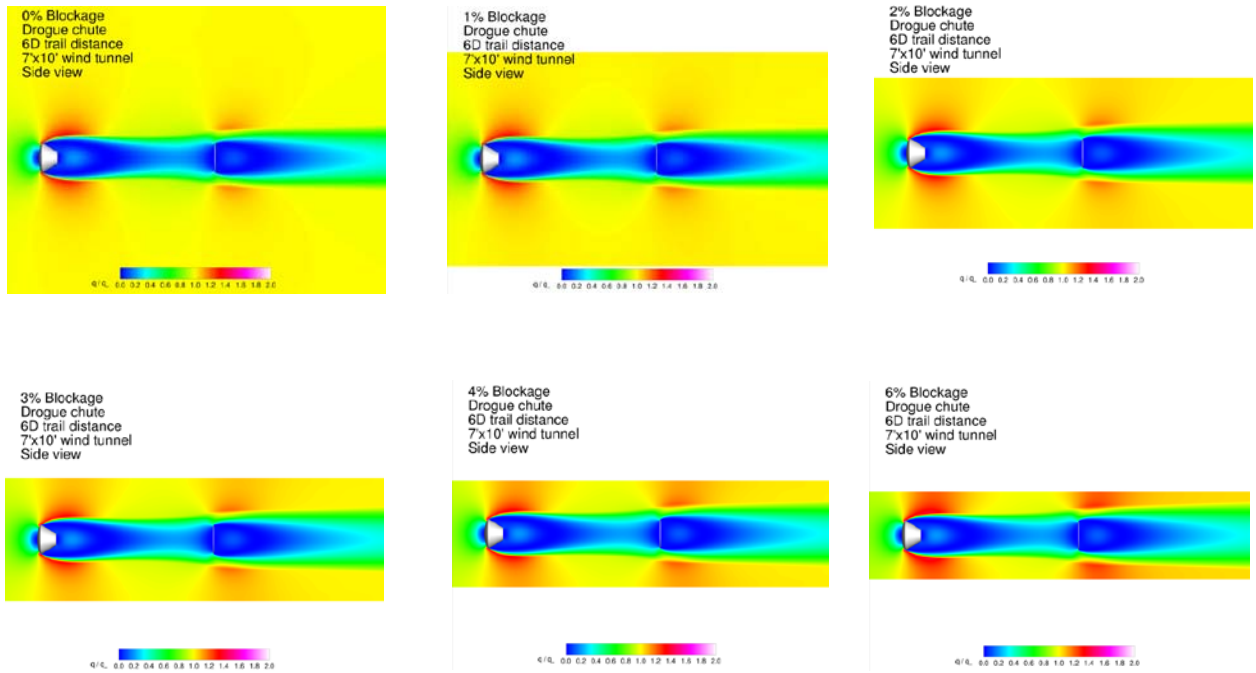


**Figure 5. Contours of normalized dynamic pressure ($q/q_{inf}$) for the CM and parachute flow field at Re=3x10$^6$ (*from left to right*) 1,2,3,4, and 6% blockage.**

## III. Test Program

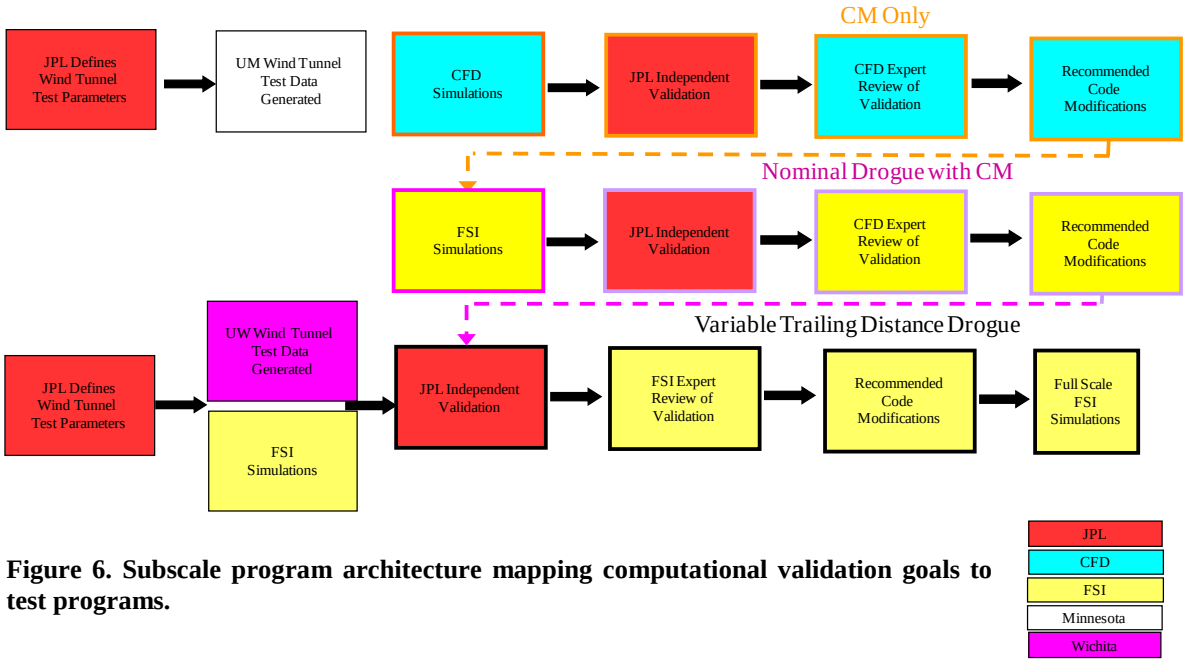


**Figure 6. Subscale program architecture mapping computational validation goals to test programs.**

A test and analysis program architecture was developed, as detailed in Figure 6. The architecture relies on a computational component, including CFD simulations to compute the CM turbulent wake and later FSI simulations to predict the parachute load and dynamic reponse. The program is divided into three phases: (1) CM alone, (2) CM with the parachute, and (3) variation in trailing distance between the CM and parachute. Each phase builds in aerodynamic and test configuration complexity. Each phase also builds on the previous one in terms of code development and validation. The first phase is being conducted at the Univeristy of Minnesota where the Particle Image Velocimetry (PIV) diagnostic is to be developed in a laboratory wind tunel. The second phase then transitions to a larger 3x2.1 m (10x7 ft) facility where a 10% scale CM is tested, with and without a 10% scale drogue parachute. The phase 3 will explore different trailing distances of the parachute behind the CM. CFD is provided by the Johnson Space Center (JSC) with the Overflow RANS solver[12] and FSI by University of Minnesota with the US3D Detached Eddy Simulation (DES) membrane solver[13].

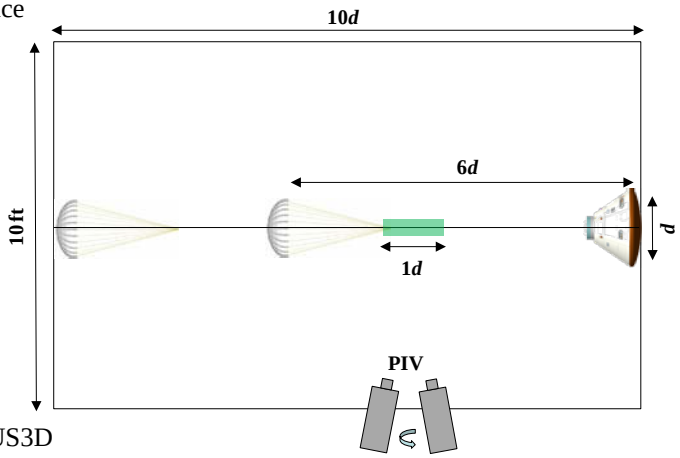


**Figure 7. 3x2.1 m test section wind tunnel layout indicating CM, parachute, laser sheet (in green), camera placement (in CM diameters).**

### A. Test Objectives

The primary objectives are to (1) quantify capsule wake upstream of the parachute, (2) quantify drogue parachute performance in the wake, (3) quantify drogue parachute inflation in the wake, (4) quantify effect of drogue trailing distance on performance, (5) generate datasets to validate CFD/FSI tools for CPAS, and (6) measure the pressure distribution within the parachute.

### B. Test Facility

Several facilities were surveyed to provide the required blockage for the drogue subscale test. Parameters of interest are test section size, open versus closed loop, maximum q, optical access, and cost. Specific requirements on the test facility were driven by obtaining similarity with *Re* number (>1.5x10$^6$) and dynamic pressure (4.8 kPa) of the CPAS drogue flight conditions and sufficient optical access for the non-intrusive measurement techniques to be discussed next. A range, from 9% to 20% of full scale, was deemed feasible from a parachute manufacturability,

image resolution, and flow seeding perspective. Table 4 summarizes a range of wind tunnel facilities that met our basic requirements and the associated scaling with each. The TAMU 3x2.1 m, open loop facility was selected and the corresponding test section layout shown in Figure 7. The added cost of the variable pressure facilities and low dynamic pressure of the Vertical Spin Tunnel (VST) eliminated those options.

**Table 4. Subsonic wind tunnel survey and scaling.**

| **Tunnel** | **Unitary**[14] | **Unitary**[14] | **Unitary**[14] | **VST**[15] | **Beech**[16,] | **Nicks**[17] | **Army**[18] | **16T**[19] |
|---|---|---|---|---|---|---|---|---|
| **Location** | GRC | GRC | GRC | LaRC | Wichita | TAMU | ARC | AEDC |
| **Test Section (m)** | 3x2.1 | 4.6x2.7 | 2.4x1.8 | 6 diam | 3x2.1 | 3x2.1 | 3x2.1 | 4.9x4.9 |
| **Variable Pressure** | Yes | No | No | No | No | No | No | Yes |
| **Max Scale (%)** | 14 | 17 | 10 | 20 | 10 | 11 | 12 | 23 |
| **Blockage (%)** | 3.9 | 4.6 | 3.9 | 1.9 | 2.9 | 3.7 | 4 | 4 |
| **TS Area ($m^2$)** | 9.3 | 12.5 | 4.5 | 37.2 | 6.5 | 6.5 | 6.5 | 24 |
| **TS Length (m)** | 12.2 | 12.2 | 4.6 | 7.6 | 3.7 | 5.5 | 6.1 | 12 |
| **Re ($x10^6$)** | 8 | 4 | 7 | 1 | 3 | 6 | 6 | 7 |
| **Max Q (kPa)** | 7 | 3 | 24 | 0 | 5 | 5 | 10 | 19 |

## C. Test Article

A ten percent scale model of the CPAS variable porosity conical ribbon (VPCR) drogue parachute is being fabricated with a geometry scaled from the flight article to the maximum extent possible. Key parameters are shown in Table 5 and compared to the full-scale article [1]. The canopy will have 24 gores, to ensure a similar inflated shape to the flight article[7]. The number of ribbons and spacing between the ribbons will vary, although maintaining the same overall geometric porosity of 19%. A preliminary stress analysis was performed to size the broadcloth, suspension lines, radials, and verticals. The canopy is made from Nylon and suspension lines and verticals from Spectra.

To reduce the complexity of manufacture, a laser cutting approach was used to create the geometric porosity, as an alternative to individual ribbons. The laser cut gore is shown in Figure 8. The parachute will also accommodate 10 pressure sensors, 5 on each of two radials, each sewn to the radial. The interface to the wind tunnel hardware will be via a textile link and swivel.

**Table 5. Subscale drogue parachute properties[1].**

| **Parameter** | **Full Scale** | **Subscale** |
|---|---|---|
| Parachute Type | VPCR | VPCR |
| $D_o$ (m) | 7 | 0.7 |
| Number of Gores | 24 | 24 |
| Number of Ribbons | 52 | 52 |
| Geometric Porosity | 19.2% | 19% |
| *x/d* | 6 | 6-10 |
| $Ls/D_o$ | 1.5 | 1.5 |
| Reefing Stages | 2 | 2 |
| *Re* ($x10^6$) | 3-10 | 1-5 |
| *q* (kPa) | 1.4-8 | 0-4.8 |
| *M* | 0.1-0.7 | 0.1-0.3 |

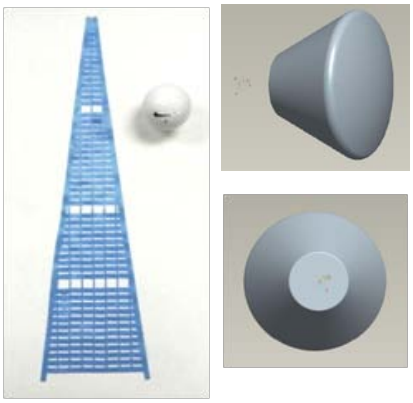

**Figure 8. (*Left*) Subscale parachute laser cut gore shown next to golf ball for scale. (*Right*) Geometry of Subscale Orion CM.**

## D. Diagnostics

Several diagnostics were reviewed and assessed with the intention of enhancing physical insight into the flow-field. They are summarized in Table 6 Minimization of aerodynamic interference and high spatial resolution is critical to generating a high quality validation dataset. Depending on the fluid dynamics of interest, time resolved measurements are also of tremendous value to capture transient effects, turbulent statistics, and dynamic behavior. Our assessment led to the selection of PIV, Kulites, and photogrammetry, as they provide the least intrusive and highest quantitative value of the set. They have also all been successfully demonstrated

in a similar environment from past NASA parachute developments[20].

*1. Particle Image Velocimetry*

Stereo PIV is a non-intrusive, spatially resolved optical measurement technique that provides three components of velocity in a planar region imaged by two cameras. The flow is seeded with tracer particles (e.g. mineral oil) and a laser light sheet illuminates the region of interest. Images of light scattered by the seed are captured by both cameras at two time steps. Velocity components are determined from the image set using cross correlation software.

**Table 6. Diagnostics survey for wind tunnel testing.**

| Diagnostic | Pressure Distribution | Wake Deficit | Drag | Stress | Dynamic Coupling |
|---|---|---|---|---|---|
| **PIV** | X | X | | | |
| **Anemometer** | | X | | | |
| **PSP** | X | | | X | |
| **Kulites** | X | | X | X | |
| **Strain Sensor** | | | X | X | |
| **Balance** | | | X | | X |
| **Load Cell** | | | X | | X |
| **Photogrammetry** | X | | | X | X |

The PIV diagnostic development is being led by the University of Minnesota (UM). In the first phase, a 1/15 scale CM model will be fabricated for the UM 0.9x1.2 m (3x4 ft) wind tunnel and interrogated with PIV. Several angles of attack will be considered at $Re \sim 3x10^5$. Stereo PIV data sets (planar fields including three velocity components) will be acquired in stream-wise/vertical planes located up to 6*d* downstream of the model. Mean and RMS velocity statistics will be obtained, in addition to analysis of typical eddy structures within the instantaneous fields. In particular, the RMS values provide insight into the magnitude of unsteadiness of the flow.

In the second phase, PIV measurements will be obtained downstream of the 10% scale CM without and with a parachute deployed in the 3x2.1 m wind tunnel faciliy. The implementation to be used in the drogue test is shown in Figures 7 and 9. Again, the two camera stereo configuration will be used to obtain planar fields with three velocity components. A pressurized air source and upstream tunnel port access for tracer particle seeding will be required. As with Phase I, most of the data will be derived from stream-wise/vertical planes located 4 to 6 *d* downstream of the model including mean, RMS, velocity statistics and instantaneous eddy structures.

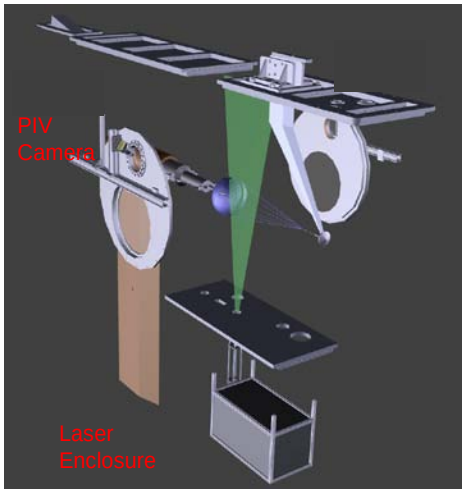


**Figure 9. Schematic of a PIV wind tunnel layout indicating laser sheet, axial interrogation region, and test article.**

*2. Pressure Measurement*

High speed pressure transducers from Kulite are to be placed on the canopy interior. The transducer layout is shown in Figure 10[21]. Each unit is less than 1.6 x 4.7 mm, weighs 0.2 grams, and provides a 0 to 5 psid range. The avionics package (amplifier) is located downstream of the transducer, to reduce the point mass on the canopy. Five Kulites will be placed on each of two radials located 90 deg apart, sewed to the canopy radial on a Delrin base plate.

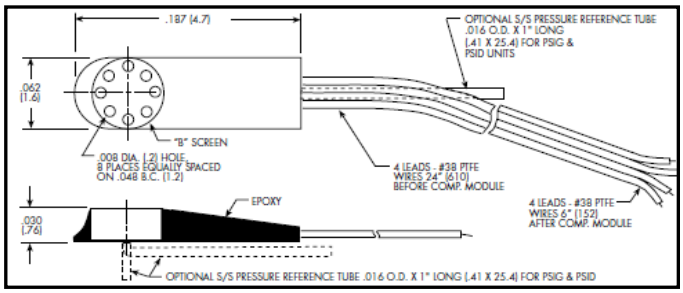


**Figure 10. Schematic of Kulite high speed pressure transducer indicating sensor head, reference tube, mounting, and cable[21].**

*3. Parachute Dynamics*

Two high speed video cameras will be used to measure the parachute dynamics and shape. Reflective targets will be placed on the canopy interior, vent, and leading edge enabling photogrammetric post-processing of area, shape, trim angle, and angular rates.

*4. Load*

A 4500-N inline load cell will measure parachute drag at >5 kHz to capture load transients and frequency content.

### E. Test Matrix

The planned test matrix is shown in Table 7. The first portion of the test matrix will measure the wake from the CM alone with PIV. This is done to compare with the initial PIV development at the University of Minnesota tunnel and to assess the usefulness of adding trip dots and/or grit to force transition to turbulence around the CM. The remainder of the test matrix will be used to explore aerodynamic dependencies of the flow field by varying Re (dynamic pressure). Non-dimensional trailing distances from 6 to 10*d* will be explored to determine the effect on wake recovery and coupling to the parachute flow. The CM angle of attack will also be varied up to 50 degrees from heat-shield forward, by a specially fitted interface mount (Figure11). Reefing will also be investigated in the context of configuration and aerodynamic response. Some configurations will be fitted with Kulites to measure the canopy pressure at 10 distinct locations, yielding the first measurement of this type for a conical ribbon canopy. The concept of operations for the test is PIV, followed by high speed video. Load and pressure transducer measurements are made continuously. For configurations that undergo a dis-reef, a PIV measurement will only be made for the first stage, due to the download time from the cameras.

**Table 7. Planned matrix for the subscale drogue wind tunnel test.**

| Test | Configuration | Kulites | Do (m) | x/d | α (deg) | $q_{inf}$ (kPa) | $Re_{max}$ | Reefing |
|---|---|---|---|---|---|---|---|---|
| A | CM only wake survey | | --- | --- | 180 | 2.4 | $2x10^5$ | --- |
| B | | | --- | --- | 150 | | | --- |
| C | | | --- | --- | 130 | | | --- |
| 1 | Parachute Only | None | 0.7 | 6 | N/A | 2.4-4.8 | N/A | No |
| 2 | | | | 10 | | | | No |
| 3 | | | | 10 | | | | Yes |
| 4 | CM with Parachute | None | 0.7 | 6 | 180 | 2.4-4.8 | $3x10^6$ | No |
| 5 | | None | | 6 | 180 | 4.8 | | Yes |
| 6 | | None | | 6 | 150 | 4.8 | | Yes |
| 7 | | None | | 6 | 130 | 2.4-4.8 | | Yes |
| 8 | | Yes | | 6 | 130 | 2.4-4.8 | | No |
| 9 | | None | | 8 | 180 | 2.4-4.8 | | Yes |
| 10 | | Yes | | 8 | 180 | 2.4-4.8 | | No |
| 11 | | None | | 10 | 180 | 4.8 | | Yes |
| 12 | | None | | 10 | 130 | 4.8 | | Yes |
| 13 | | Yes | | 10 | 180 | 4.8 | | No |

## IV. Systems Engineering Benefits

The final aspect of the study is a survey of the systems level benefits that this approach achieves, including reduction in load prediction, mass allocation, and potential for drag performance improvements, as well as risk mitigation for a full-scale development.

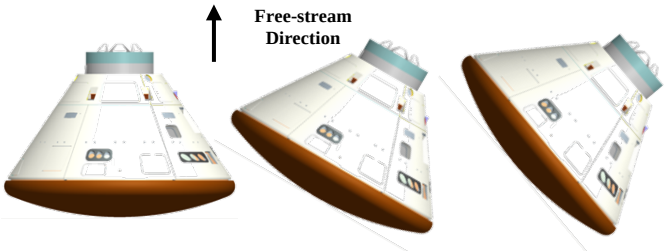


**Figure 11. Pitch plane angles of the CM to be investigated in the subscale test program are (from left to right) α=180, 150, 130 deg. 180 deg is the orientation with the heat-shield pointing into the flow.**

Parachutes are typically designed with design utilization factors in excess of 2 due to a combination of textile, environmental, and load distribution knock-down factors[7]. In addition, canopy stress is based on an unknown pressure distribution, and peak load on a drag coefficient measured in the wake of a stream-lined test vehicle. In the wake of a blunt body payload drag is typically reduced due to flow separation upstream of the parachute. Similarly, pressure distribution is likely not uniform. If these factors can be better quantified, the nominal stress distribution can be more accurately calculated, and incorporated into the textile sizing. A reduction in ribbon weight, suspension line diameter, or riser size can lead to a reduction in mass and volume for the overall parachute system. From typical sizing factors this could translate into a 10 to 20% reduction in mass.

In addition to decreasing steady state drag, aerodynamic interactions with the payload may also create transients and load overshoots that need to be factored into the textile sizing. Without a quantification of these transients, the parachute designer has little choice but to add additional qualitative margin. The result is a sizing that is not mass optimized, and perhaps insufficient. Quantifying the true flight environment ultimately reduces risk in the development phase. Similarly, a mature basis for the mass allocation reduces the potential for future mass and volume growth, critical to entry and recovery systems.

## V. Conclusion

A subscale test program to measure the Orion drogue performance is underway. The program will measure the spatially and temporally resolved velocity field upstream of the parachute with PIV, pressure distribution inside of the canopy with transducers, parachute dynamics with high speed video, and time resolved drag with a load cell. A test facility and diagnostics suite have been selected to this end. A quantitative approach to the test design that utilizes CFD to design the experiment has been implemented. Simulations of the test configuration have been performed to provide load estimates for tunnel support hardware and an acceptable level of blockage. Ten percent scale test articles are under fabrication using a novel laser cutting approach to provide maximize similarity to the full-scale inflated shape and geometric porosity. A test matrix that explores trailing distance, *Re*, and CM angle of attack will provide new insight into the CPAS drogue performance.

## Acknowledgments

The authors would like to acknowledge the support of Justin Johnson from Airborne Systems. This work was carried out at the Jet Propulsion Laboratory, California Institute of Technology, under a contract with the National Aeronautics and Space Administration.

## References

[1] R. Olmstead et. al., "Overview of the Crew Exploration Vehicle Parachute Assembly System (CPAS) Generation I Drogue and Pilot Development Test Results," AIAA-2009-2939, 20th AIAA Aerodynamic Decelerator Systems Technology Conference and Seminar, 4 - 7 May 2009, Seattle, WA.

[2] D. Lichodziejewski et. Al., "Development and Testing of the Orion CEV Parachute Assembly System (CPAS)," AIAA-2009-2938, 20th AIAA Aerodynamic Decelerator Systems Technology Conference and Seminar, 4 - 7 May 2009, Seattle, WA.

[3]D.E. Reichenau,."Aerodynamic Characteristics of Disk-Gap-Band Parachutes in the Wake of Viking Entry Forebodies at Mach Numbers from 0.2 to 2.6," AEDCTR72-78, 1972.

[4]J. Barber and H. Johari, Experimental Investigation of Personnel Parachute Designs Using Scale Model Wind Tunnel Testing," AIAA 2001-2074.

[5] J. Cruz et. al., "Wind Tunnel Testing of Various Disk-Gap-Band Parachutes," AIAA 2003-2129.

[6]A. Sengupta et. al., "Results from the Mars Science Laboratory Parachute Decelerator System Supersonic Qualification Program," Proc. of the IEEE 2008 Aero Con, March 2008.

[7] T.W. Knacke, *Parachute Recovery Systems Design Manual*, Para Publishing, Santa Barbara, CA, 1992.

[8] Ricardo A. Machin1 and Carol T. Evans. "Cluster Development Test 2 an Assessment of a Failed Test," AIAA-2009-2902, 20th AIAA Aerodynamic Decelerator Systems Technology Conference, May 2009, Seattle, WA.

[9] E.R. HiZGe, "Entry Flight Aerodynamics from Apollo Mission AS-202," NASA TN D-4185, October 1967.

[10] D. Sahini, "Wind Tunnel Blockage Corrections: A Computational Study," Graduate Thesis, Mechanical Engineering Dept., Texas Tech University, August 2004.

[11] E.C. Maskell, "A Theory of the Blockage Effects on Bluff Bodies and Stalled Wings in a Closed Wind Tunnel, " R.A.E. Report No. 3400, November 1963.

[12] R.H. Nichols, R.W. Tramel, P.G. Buning, "Solver and turbulence model upgrades 435 to OVERFLOW 2 for unsteady and high-speed applications," AIAA-2006-436 2824, AIAA.

[13] V. Gidzak et. al., "Simulation of Fluid-Structure Interaction of the Mars Science Laboratory Parachute," AIAA-2008-6910 , 26th AIAA Applied Aerodynamics Conference, Honolulu, Hawaii, Aug, 2008.

[14] http://facilities.grc.nasa.gov/documents/TOPS/TopWindTunnels.pdf.

[15] http://gftd.larc.nasa.gov/references/VST_factsheet.pdf.

[16] http://www.niar.twsu.edu/researchlabs/pdf/Lab%20info%20sheets/WindTunnel_Handout.pdf.
[17] http://lswt.tamu.edu/download.htm#Facility_Handbook.
[18] http://rotorcraft.arc.nasa.gov/Publications/files/Silva_AHS04.pdf.
[19] http://www.arnold.af.mil/library/factsheets/factsheet.asp?id=13714.
[20] A. Sengupta et. al., "Findings from the Supersonic Qualification Program for the Mars Science Laboratory Parachute System" 20th AIAA Aerodynamic Decelerator Conference, Seattle, WA May 4-8th 2009.
[21] http://www.elsensors.com/html/kulite/LQ.LE-062.pdf.